EGG-M--91247

DE92 003271

INTERPRETATION OF EXPERIMENTAL RESULTS FROM THE CORA CORE MELT PROGRESSION EXPERIMENTS[a]

J. K. Hohorst and C. M. Allison
Idaho National Engineering Laboratory
EG&G Idaho, Inc.
Idaho Falls, ID 83415
(208) 526-9414, 526-9009

ABSTRACT

Data obtained from the CORA bundle heatup and melting experiments, performed at Kernforschungszentrum, Karlsruhe, Germany, are being analyzed at the Idaho National Engineering Laboratory. The analysis is being performed as part of a systematic review of core melt progression experiments for the United States Nuclear Regulatory Commission to (a) develop an improved understanding of important phenomena occurring during a severe accident, (b) to validate existing severe accident models, and (c) where necessary, develop improved models.

An assessment of the variations in damage progression behavior because of variations in test parameters (a) bundle design and size, (b) system pressure, (c) slow cooling of the damaged bundles in argon versus rapid quenching in water, and (d) bundle inlet temperatures and flow rates is provided in the paper. The influence of uncertainties in important test conditions is also discussed. Specific results presented include (a) bundle temperature, (b) the onset and movement of the oxidation front within the bundle, (c) fuel rod ballooning and rod failure, and (d) melt relocation and associated material interactions between bundle components and structures.

INTRODUCTION

Data obtained from the CORA bundle heatup and melting experiments,[1,2,3] performed at Kernforschungszentrum, Karlsruhe, Germany, are being analyzed at the Idaho National Engineering Laboratory. These experiments, which systematically vary test conditions important to core melt progression processes, are being analyzed for the United States Nuclear Regulatory Commission to (a) develop an improved understanding of important phenomena occurring during a severe accident, (b) to validate SCDAP/RELAP5[4] severe accident models, and (c) where necessary, develop improved models.

An assessment of the variations in damage progression behavior due to variations in test parameters (a) bundle design and size, (b) system pressure, (c) slow cooling of the damaged bundles in argon versus rapid quenching in water, and (d) bundle inlet temperatures and flow rates is provided in the paper. The influence of uncertainties in important test conditions is also discussed. Specific results presented include (a) bundle temperature, (b) the onset and movement of the oxidation front within the bundle, (c) fuel rod ballooning and rod failure, and (d) melt relocation and associated material interactions between bundle components and structures.

Table 1 summarizes the tests considered and the variations in test conditions, parameters, and bundle geometry between each test. Table 2 summarizes the objectives of each test.

DESCRIPTION OF THE CORA FACILITY AND CONDITIONS

The CORA facility test section, illustrated in Figure 1, incorporates a representative 2-m-high fuel rod bundle with a 1-m electrically heated region that simulates decay power. PWR and BWR bundle configurations, Figure 2, consist of simulator heater rods, unheated fuel rods, and control material, Ag-In-Cd (silver-indium-cadmium) control rods or a B_4C (boron carbide) control blade surrounded by an insulating shroud. The insulating shroud consists of a zircaloy liner surrounded by a porous zirconia insulation into which windows at various elevations are cut to allow viewing and video recording of bundle damage progression during an experiment. All structures above the 1471-mm level and below the -250-mm level in

[a]Work supported by the U.S. Nuclear Regulatory Commission, Office of Research, under DOE Contract No. DE-AC07-76ID01570.

Paper submitted for presentation in the Thermal Hydraulics of Severe Accidents session of the Winter Meeting of the ANS in San Francisco, November, 1991.

TABLE 1. Summary of CORA Experiments and Test Conditions

Test	Bundle Type	Rod Bundle Size	Control Material	Number of Rods or Blades	Bar Pressure	Type Cladding	Maximum Temperature (K)
CORA-2	PWR	25	None	0	1	Slow	2050
CORA-5	PWR	25	Ag-In-Cd	1	1	Slow	2300
CORA-7	PWR	57	Ag-In-Cd	5	2	Slow	2100
CORA-9	PWR	25	Ag-In-Cd	2	10	Slow	2100
CORA-12	PWR	25	Ag-In-Cd	2	2	Quench	2100
CORA-15	PWR	25	Ag-In-Cd	2	2	Slow	2100
CORA-16	BWR	18	B_4C blade	1	2	Slow	2100
CORA-17	BWR	18	B_4C blade	1	2	Quench	2100
CORA-18	BWR	48	B_4C blade	1	2	Slow	2100

TABLE 2. Objectives of the CORA Tests

Test	Objective
CORA-2	A reference test using no absorber material to observe the interaction between the zircaloy cladding on the fuel rods and the inconel grid spacer.
CORA-5	A test to evaluate the effects of absorber material on core damage and to observe the effects of a higher end temperature.
CORA-7	To examine the influence of a larger bundle on the damage experienced by the fuel rods in the bundle.
CORA-9	To test the influence of a higher system pressure on the damage experienced by the fuel rods in the bundle
CORA-12	To test the influence of quench cooling during small bundle PWR test using absorber material.
CORA-15	To test the influence of ballooning and bursting of the cladding on the damage experienced by the bundle.
CORA-16	To observe the interactions that occur between the B_4C absorber material and the stainless steel of the control blade and then the stainless steel from the blade with zircaloy from the channel box.
CORA-17	To observe the effects of quenching on a BWR test as CORA-16. The test conditions were the same as CORA-16 up to quench.
CORA-18	To observe BWR bundle size effects on damage experienced by the fuel rods in the bundle.

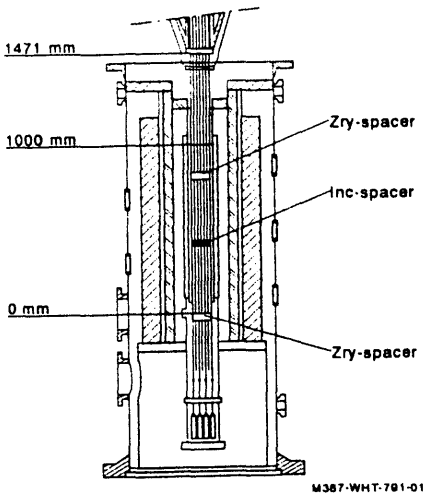

Fig. 1. Schematic of the CORA PWR test section.

the bundle are cooled to near room temperature by water.

The electrically heated simulator rods used in all CORA tests are of typical PWR size and consist of a central tungsten heater element surrounded by annular uranium dioxide pellets clad with zircaloy. The number of heater rods used in an experiment depend on bundle size and/or configuration. Typically, a small bundle PWR (25 rods total) test used 16 heated rods, a small bundle BWR (18 rods) used 12, a large bundle PWR (57 rods) test used 32, and a large bundle BWR (48 rods) test used 28. The unheated rods for all tests are of typical PWR size and consist of a zircaloy cladding surrounding solid UO_2 pellets. The absorber rod used in the CORA PWR tests consisted of a stainless steel clad, Ag-In-Cd absorber rod surrounded by a zircaloy guide tube. The BWR CORA experiments incorporated a rectangular zircaloy structure representing BWR fuel canister walls. This structure enclosed a representative stainless steel clad, B_4C control blade.

Test Procedure

The procedure used for each test consisted of the following steps. A week prior to the experiment, a pretest heatup was conducted using the expected initial conditions for the test. The bundle was allowed to heat at a rate of 1 K/s until a temperature between 900 and 1000 K was measured in the bundle. Initial conditions, early heatup rates, and instrumentation were checked during this phase. The night before the test, argon at approximately 1000 K was circulated through the bundle for at least 12 hours to bring the bundle components and flowing gas to thermal equilibrium. The transient was then initiated by applying electrical power to the heater rods with continued argon flow. Superheated steam was introduced into the bundle either when power to the heater rods was initiated or 300 s after the initiation of power to the heater rods. A steam-argon mixture flowed through the bundle for a predetermined period of time as power to the heater rods was linearly increased. The steam flow was then terminated and the system allowed to continue heating until the desired peak temperature was attained. At this time, power to the heater rods was terminated and the system allowed to cool either gradually or by quenching. If a quench was employed, the positioning of the quench tank over the bundle started either after the power transient or 30 s before power to the heater rods was terminated. Throughout the tests, conditions were recorded

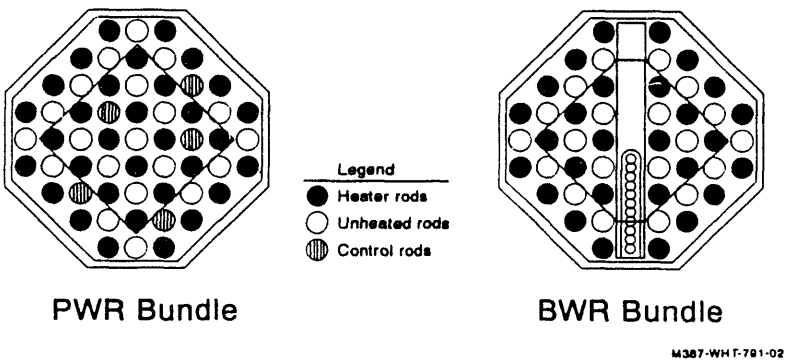

Fig. 2. Cross-sections of a PWR and BWR configured CORA bundle.

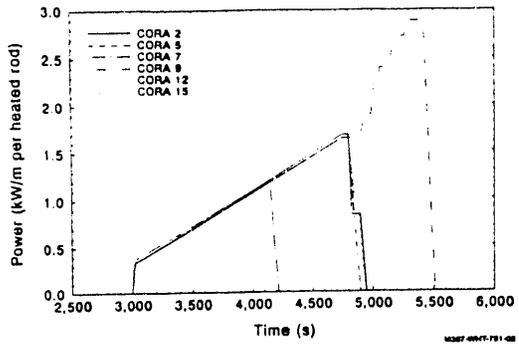

Fig. 3. Input power in kW/m per heated rod for the small and large bundle PWR tests.

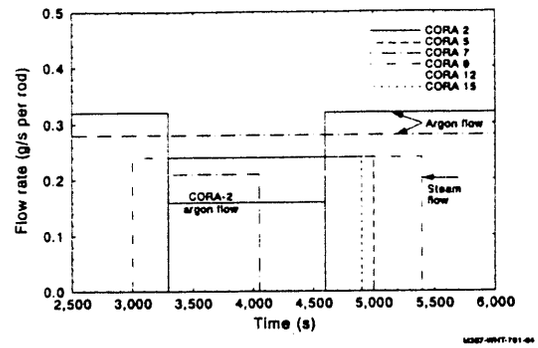

Fig. 4. Argon and steam mass flow rates in g/s per rod for the small and large bundle PWR tests.

and monitored by a data acquisition system. Damage progression occurring in the bundle was viewed and recorded using video monitors. Upon completion of the test the bundle was sliced into small sections and a metallurgical examination performed.

Boundary Conditions

Argon or argon/steam mixture was injected into the bottom of the bundle. Figures 3 and 4 show the mixture flow rates, along with bundle electric power, used for the CORA PWR tests. Figure 5 shows the conditions used for the BWR tests. The mixture was heated to 1000 K in a superheater but cooled as it moved into the inlet of the bundle. The amount of cooling was dependent on the total mass flow rates of coolant flowing through the pipe and the system pressure during the experiment. Figures 6 and 7 show the resulting inlet temperatures.

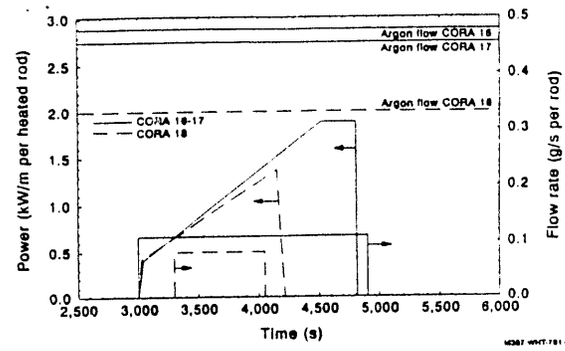

Fig. 5. Input power in kW/m per heated rod and argon and steam flow rates in g/s per rod (heated and unheated) for the small and large bundle BWR experiments.

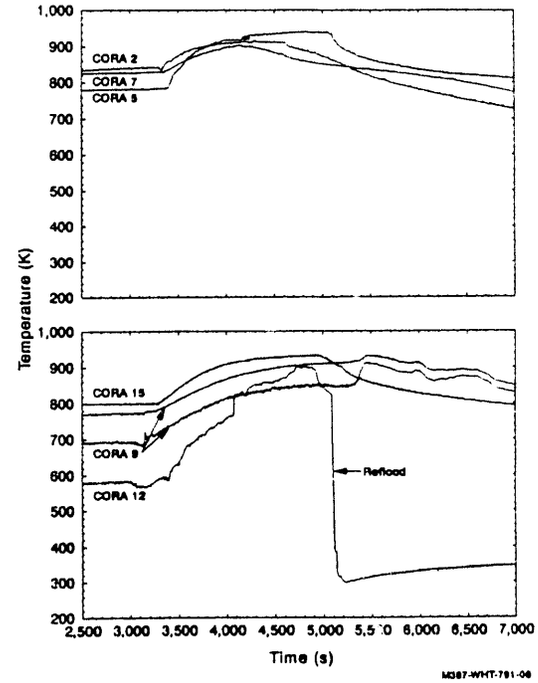

Fig. 6. Measured bundle inlet temperatures for the PWR experiments.

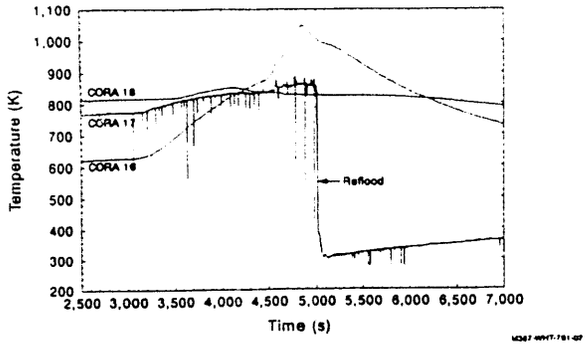

Fig. 7. Measured bundle inlet temperatures for the BWR experiments.

The coolant gas flows (steam and argon) into the bundle were scaled to provide consistent and equivalent convective cooling for the different bundle sizes. The one notable exception was the CORA-2 PWR test. In CORA-2, the argon flow rate was reduced well below that of the other PWR tests at the time steam flow was introduced into the bundle. The total argon and steam flow was approximately the same for the PWR and BWR tests. However, the argon flow per rod in the BWR tests was greater than for the PWR tests while the steam flow per rod was less. The steam flow was adjusted to a value representative of postulated BWR accident conditions. The duration of steam flow varied from test to test, but the most common pattern was from 300 s after the initiation of power to the rods to the end of the power transient.

Power to the heater rods was increased linearly with time to develop a heatup rate equal to 1 K/s up to the onset of rapid oxidation and a maximum bundle temperature between 2100 and 2300 K. For all tests with the exception of the two large bundle tests, CORA-7[5] and 18, and the high system pressure test, CORA-9, the power histories were identical. In the CORA-7[5] and CORA-18 tests, the desired peak bundle temperatures were reached at a power per rod significantly below that of the smaller bundle tests. In the high system pressure test, CORA-9, the power history was identical to all other tests up to 5000 s. However since bundle temperatures were considerably less than in other tests, power was increased dramatically to induce bundle heatup.

TEST RESULTS

Bundle Temperatures

Inlet coolant temperature varied from test to test as shown in Figures 6 and 7. This variation in temperature was attributed to slight differences in boundary conditions, bundle pressure, or to the duration of bundle pretest heating. The lower than expected measured temperatures for the CORA-12 and CORA-16 tests were attributed to a shorter preheat phase than used in the other tests and possible measurement error.[6] The cause for the lower inlet temperature for the CORA-9 test has not been reported.

Figures 8, 9, and 10 show measured temperatures at three separate bundle elevations. Near the bottom of the bundle, 350 mm from the inlet, temperatures for all tests, except the high system pressure test CORA-9, were within 75 K during the initial heatup phase with CORA-7, the large bundle PWR test, being the hottest. By the time the coolant had reached this elevation, the effect of the observed variations in inlet temperatures had little effect on the progression of the tests. The largest variation in bundle behavior began near

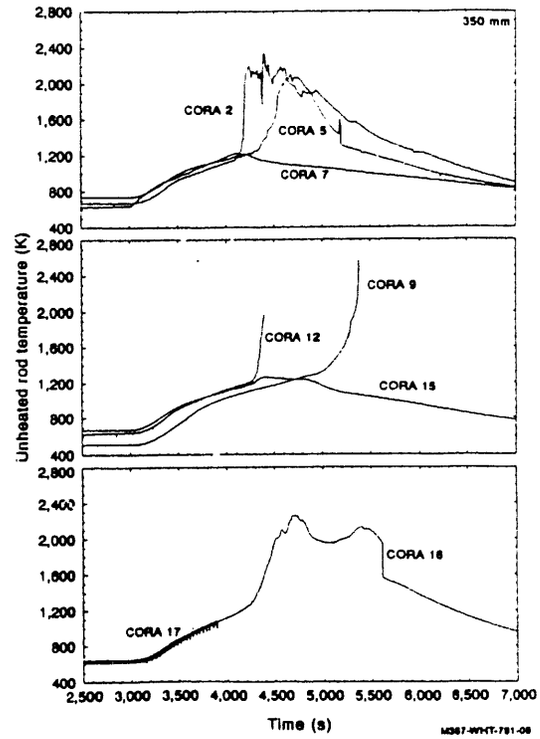

Fig. 8. Measured unheated fuel rod temperatures at the 350 mm elevation in the bundle.

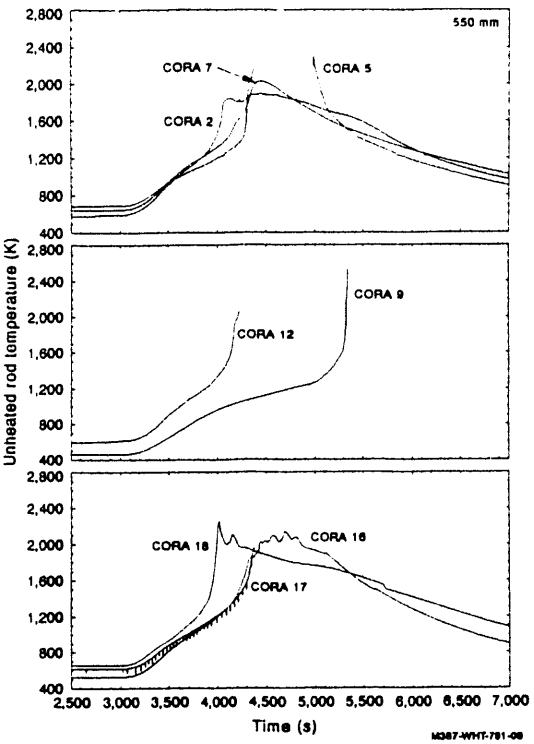

Fig. 9. Measured unheated fuel rod temperatures at the 550 mm elevation in the bundle.

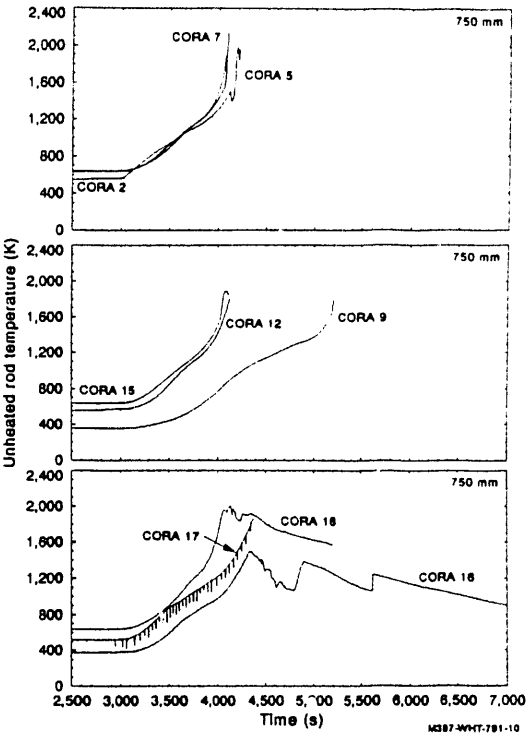

Fig. 10. Measured unheated fuel rod temperatures at the 750-mm elevation in the bundle.

4100 s, when molten material relocating from higher elevations in the bundle came in contact with the mounted thermocouples, resulting in a sharp rise in temperature. Two experiments, CORA-7 and CORA-15, showed little variation in temperature at the 350-mm elevation, indicating that (a) rapid oxidation did not occur at this elevation and (b) the hot molten material that moved downward from the upper portions of the bundle did not reach this elevation. Up to 4100 s, at the 350-mm elevation, the CORA-9 fuel rod heatup rate is similar to the other CORA tests but with the measured temperature consistently 125 K cooler during the early phases of the transient. At 4100 s, the fuel rod heating rate in CORA-9 decreased to 0.28 K/s. Heating continued at this rate until shortly after the increase in electrical power to the heated rods when a fuel rod temperature of 1300 K was attained and run away oxidation of bundle zircaloy began.

At the 550-mm elevation, the initial temperature response is similar to what is observed at the lower elevation, CORA-7 being the hottest and the high system pressure test, CORA-9, about 150 K cooler. The temperature response of the PWR and small bundle BWR tests, with the exception of CORA-2 and CORA-9, were consistent with each other. CORA-2, with no absorber material and less coolant flowing through the bundle, showed a more rapid rise in temperature because of rapid oxidation. At the 550-mm elevation, CORA-9 fuel rod heating, though starting at a comparable transient time with measured temperatures 150 K cooler, progressed at rates slightly slower than observed in the other CORA tests. At 4100 s when the low pressure CORA tests had started rapid bundle oxidation, CORA-9 heatup rates slowed further. This slow and gradual heatup of the CORA-9 fuel rods continued until electrical power to the heated rods was increased at a transient time of 5000 s. Shortly after the rod power was increased, a fuel rod temperature of 1300 K was measured and rapid oxidation of the bundle zircaloy began.

Comparing the temperature response of the large bundle BWR test, CORA-18, with the

corresponding large bundle PWR test, CORA-7, it was observed in the BWR test that an initial hot spot occurred near the zircaloy grid spacer, causing rapid oxidation to begin earlier and lower in the bundle.

At the 750-mm elevation in the bundle, initial temperature measurements and heatup rate histories are similar to those at lower elevations. CORA-16 is a notable exception. The measured temperature on an unheated rod at this elevation exhibits anomalous behavior with the temperature approximately 150 K lower than other rods either in the same bundle or in the companion CORA-17 bundle.

Fuel Rod Ballooning and Rod Failure

Figure 11 shows the ballooning process in fuel rods graphically. During the CORA-2 test, ballooning began at temperatures near 1000 K when the internal pressure in the fuel rods exceeded the system pressure. The balloons continued to grow over 500 s, until the strain developing on the fuel rod cladding between the 0.55- to 0.7-m elevations became large enough to cause the rods to burst. The ballooning behavior in the CORA-15 test with a much higher internal fuel rod pressure, was considerably different. In CORA-15, ballooning began between the 0.4- and 0.8-m elevations at temperatures near 1300 K. Cladding strains developed quickly with the rods bursting in less than 100 s.[7] CORA-7 showed some ballooning or fuel rod deformation occurring at temperatures near 1300 K. The cladding deformation was not sufficient to cause the fuel rods to fail.

Onset and Movement of the Oxidation Front

The graphical representation of the zircaloy oxidation front provided in Figure 12 shows that oxidation began slowly at temperatures near 1400 K in both the PWR and BWR tests and moved through most of the bundle. When the bundle temperature reached 1500 K, rapid oxidation began in the upper quarter of the bundle for a PWR configured test and at the middle, near the zircaloy grid spacer, in a BWR configured bundle. In the PWR tests, the oxidation front moved quickly upward oxidizing the zircaloy in the upper plenum and then downward to the lower quarter of the bundle. In the BWR tests, the oxidation front moved upward toward the upper plenum, and downward from the onset point a short distance. A larger quantity of zircaloy fuel rod cladding in a PWR bundle oxidized, but because of the larger quantities of structural zircaloy in the BWR bundle, hydrogen production for similar size test bundles were similar.

Melt Relocation and Material Interactions

Figure 11 shows the relationship between the measured temperature and bundle location where the melt relocation occurred. Figure 13 shows the location and temperatures at which interactions occurred between different materials in the bundle.

The video recordings show that in BWR tests, the control blade started melting at 1550 K, well below the melting temperatures of stainless steel and B_4C, and then relocated quickly to the lower, cooler sections of the

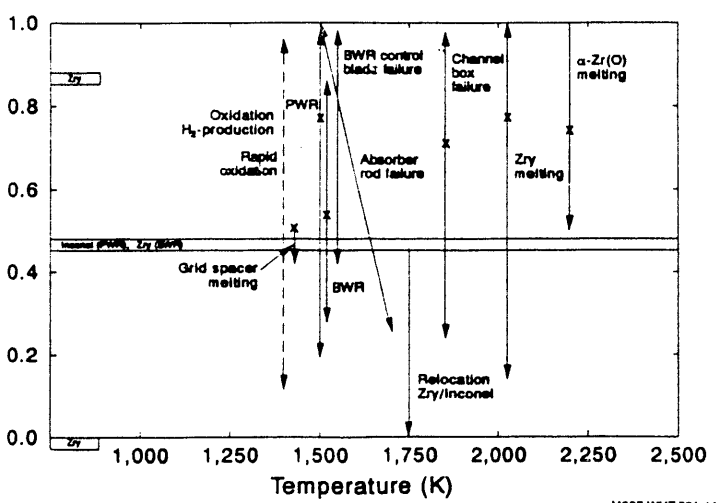

Fig. 11. Graphical representation of fuel rod ballooning that occurs in a test bundle.

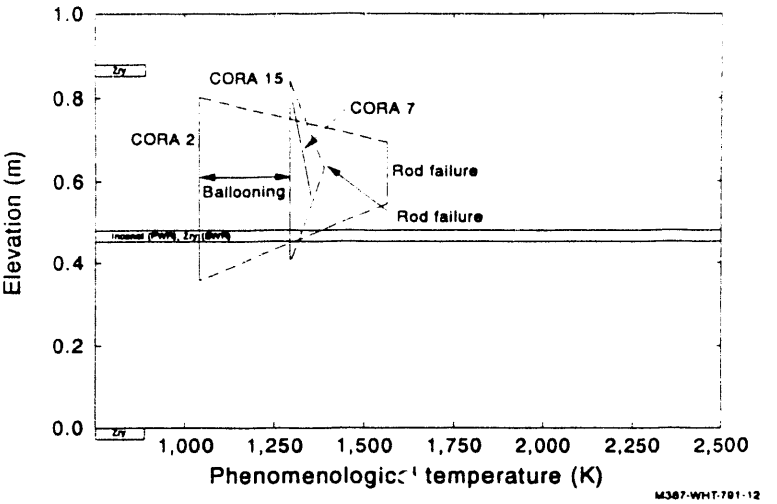

Fig. 12. PWR and BWR bundle relocation phenomena occurring during a severe accident.

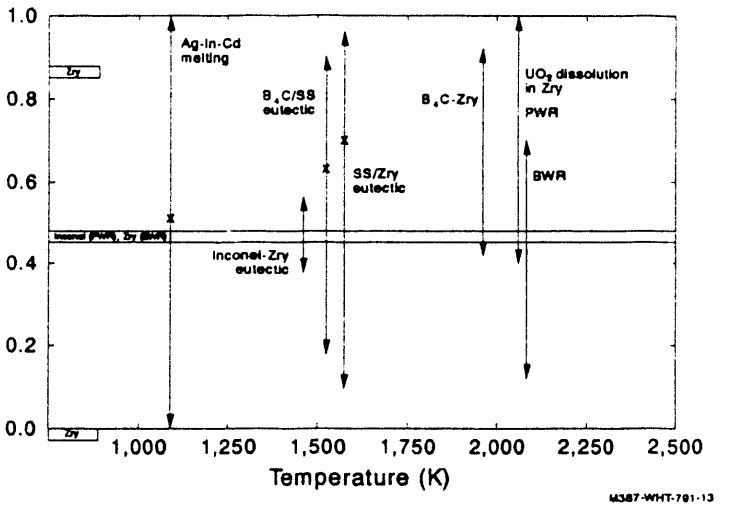

Fig. 13.' Typical locations of material interactions occurring in PWR and BWR bundles.

bundle. This quick relocation to the bottom of the bundle was also noticed when the channel box failed. Interactions between the zircaloy of the channel box and molten stainless steel from the control blade, caused complete channel box failure to occur at temperatures near 1575 K.[8] The initial hot spot in the bundle occurred near the middle and interactions began first between the zircaloy grid spacer and the zircaloy of the channel box and fuel rod cladding.

In the PWR tests, the melt relocation process was initiated by the failure of the stainless steel cladding of the Ag-In-Cd absorber rods. Ag-In-Cd melts at 1073 K. Since

this alloy does not react with its stainless steel cladding, it remained as a molten mass in the tube until interactions between the stainless steel and guide tube zircaloy resulted in cladding failure. Once the stainless steel cladding failed, interactions between the absorber material and zircaloy occurred, though they were not as prominent as other interactions that occurred. Once material interactions between zircaloy, stainless steel, and Inconel of the grid spacer began, rapid deterioration of the grid spacer occurred, with grid spacer material completely relocating downward in the bundle at temperatures between 1450 to 1500 K. Failure of the absorber rods occurred slower than for control blades in the BWR tests. The PWR control rods failed over a temperature range of 150 K,[8,9,10] starting near the initial bundle hot spot, 0.75 m, at a temperature of 1500 K. Complete absorber rod failure occurred when the stainless steel casing of the absorber material came in contact with the zircaloy guide tube, either by the movement of the stainless steel tube from its centered position or by expansion of the tube because of the formation of cadmium vapor, causing failure of the rod. The interactions between stainless steel, Inconel, and zircaloy were confirmed by the posttest metallurgical examination of the damaged bundle.

Data from posttest metallurgical examinations also indicated that the maximum amount of fuel was dissolved by liquefied fuel rod zircaloy from the upper bundle in PWR configured tests and from the middle bundle regions in BWR configured tests.

The video records of the CORA tests showed that melting and the subsequent relocation to lower and cooler elevations in the bundle occurred predominantly by droplet formation or rivulet flow. Figure 14 compares the observed bundle elevations and relocation mechanisms of two different CORA tests, the CORA-15 small bundle PWR test and the CORA-17 small bundle BWR test. Both tests used the same power history and similar total coolant flows through the bundle during the test.[12] In the CORA-15 test, a frontal movement of the bundle melting was observed during the test. Melt in the form of rivulets, which flowed downward, and falling droplets of clad and absorber material were observed to form first near the 0.75-m elevation and then at progressively lower elevations in the bundle over a period of 400 s. In the uppermost sections of the bundle rivulet flow was most prominent. Lower in the bundle, near the 0.55-m elevation, during the initial stages of melt relocation, relocation occurred as combination of rivulet flow and falling droplets. Later in the sequence, near the end of the transient and at the 0.45-m elevation, the predominant relocation mechanism was observed to change to falling drops.

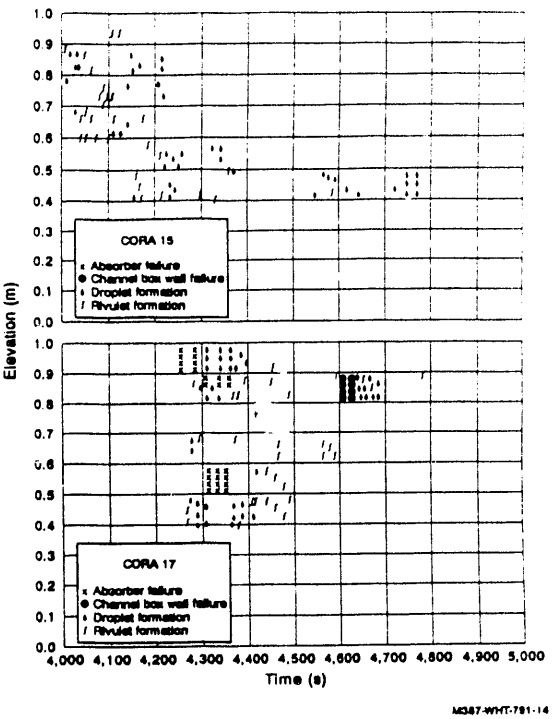

Fig. 14. Rivulets and droplets are formed during the relocation process in PWRs and BWRs.

Melt relocation in the CORA-17 BWR bundle began near the middle of the bundle with the melting of control blade materials progressing quickly upward and downward a short distance. Complete melting and relocation of the upper portions of the control blade occurred within a few seconds. The first indication of any relocation other than control blade melting, occurred near the 0.6-m elevation with the formation of droplets and a few rivulets of cladding which relocated immediately to the bottom of the channel box. After the relocation of control blade material, rivulets and droplets of cladding material formed simultaneously at all upper bundle elevations and flowed freely downward. Melt progression occurred with no indication of the formation of an oxidation front as was observed in the PWR case. The quick relocation process in the BWR can be attributed to the initial hot spot forming in the middle of the bundle and to the large flow areas available for flowing melt to pass through. The first observed melt relocation process of the fuel rod cladding was the formation of droplets near the middle of the bundle,

which quickly changed to rivulet flow when the control blade disappeared. Rivulets with a few intermixed droplets were observed at all elevations through the viewing windows until channel box failure at 1575 K, when droplets forming near the middle of the bundle were again observed to be the predominant method of relocation.

Information obtained from posttest metallurgical examinations in combination with visual and temperature data from the experiments was used to develop a composite picture of a bundle end-state. Figure 15 shows the end-states of three PWR bundles, one with no absorber material, CORA-2, one with a single Ag-In-Cd control rod, CORA-5, and one with two Ag-In-Cd control rods, CORA-12 and a typical BWR bundle, CORA-16. In the CORA-2 test, a small blockage was formed at the bottom of the bundle, though most material relocated and solidified forming a partial blockage near the 0.35-m elevation. In the CORA-5 and 12 tests, the major blockage occurred in the vicinity of the Inconel grid spacer, with a small amount of molten material flowing through and solidifying near the 0.35-m elevation. In the CORA-16 test, the major blockage formed at the bottom of the bundle.

Figure 16 shows a comparison between the end-states of a typical PWR bundle and a BWR bundle. Posttest analysis of the BWR bundles, from the CORA-16, 17, and 18 tests showed that most material relocated to the bottom of the bundle, as shown in the figure. In a typical PWR bundle, the major blockage was formed in the vicinity of the Inconel grid spacer with a smaller blockage being formed near the 0.35-m elevation. UO_2 dissolution in molten zircaloy occurred in the upper half of the PWR bundles and in the middle half of the BWR bundles corresponding to the location of the initial hot spot in the bundles.

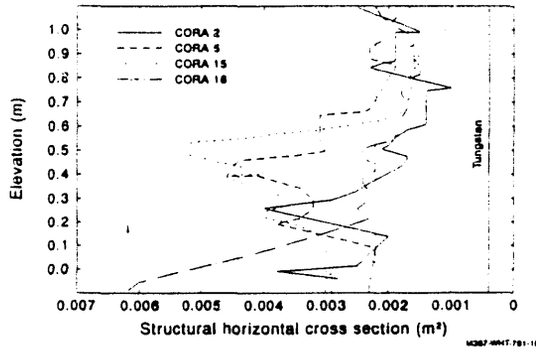

Fig. 15. Observed variations in bundle end-states for bundles with different (PWR and BWR) configurations.

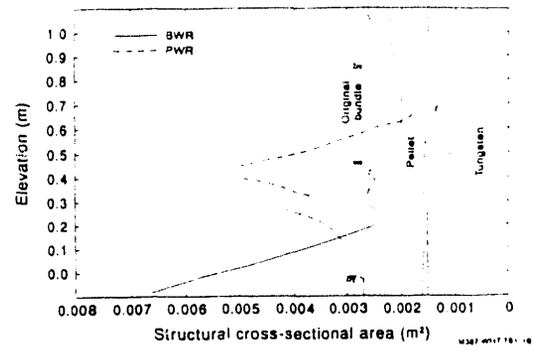

Fig. 16. A comparison between PWR and BWR relocation and fuel dissolution.

CONCLUSIONS

The ease of changing bundle configurations, controlling boundary conditions, and visually observing bundle behavior during a test, make the CORA experiments an extremely valuable tool in assessing severe accident computer codes, as SCDAP/RELAP5, and evaluating phenomena occurring in a reactor core during a severe accident. In the CORA experiments the bundle design and test conditions were systematically varied during the experiments to quantify the influence of key parameters on core melt progression including (a) bundle design and size, (b) system pressure, (c) slow cooling of the damaged bundles in argon versus rapid quenching in water. However, in many cases it was not possible to control all of the test conditions precisely due to operational constraints or experimental uncertainties. Variations in bundle inlet temperatures, flow rates, and heat losses were the most obvious and in some cases introduced significant uncertainties into the interpretation of the results.

Bundle Design and Size

Comparisons made between the various tests showed that the addition of absorber material to the bundle, either Ag-In-Cd control rods in a PWR configured bundle or a B_4C control blade in a BWR configured bundle, affected the course of melt progression in the bundle because of the presence of additional unheated material in the bundle. As a result the onset on rapid oxidation was delayed from comparable bundles without absorber material. In a BWR configured bundle, the delayed onset of rapid oxidation was more prominent because of the relatively larger mass associated with the control blade and channel box as compared to PWR control rods.

The addition of absorber material also effected the end-state of the bundle. Material interactions occurring between the stainless steel cladding, absorber material, zircaloy guide tube, and grid spacers, Inconel or zircaloy, caused material to liquefy at temperatures lower than their individual melting temperatures. In the PWR tests where Ag-In-Cd absorber rods were used, material liquefied near the top of the bundle and flowed downward, slowing and solidifying near the Inconel grid spacer resulting in a large flow blockage region. In some cases, if temperatures were sufficiently high, a small quantity of material continued to flow downward forming a smaller blockage below the spacer grid. In the BWR tests, material liquefaction started in the middle of the bundle but quickly involved the upper portions as well. B_4C and stainless steel relocated quickly to the bottom of the bundle, first filling the channel box and then spreading out to fill all available space between adjacent fuel rods, forming a major blockage region at the bottom of the bundle. Even though direct comparison was confused by a difference in coolant flow rates, the flow blockage region in CORA-2, a test without control material, formed midway between a typical PWR and BWR bundle. The observed differences in the bundle end-state indicate that the differences in heatup rates, measured temperatures at the same elevation, timing of relocation phenomena, and material interactions occurring between bundle components can be directly correlated to the bundle configuration or to the type and amount of absorber material contained in the bundle.

PWR bundle size appeared to have a small effect on the maximum heating rates in the bundle up to 1773 K. The identical bundle thermal response observed in the CORA-5, 7, 12, and 15 tests at the 550- and 750-mm elevation, showed that bundle size had little influence on the heatup behavior in the upper portions of the bundle, though differences in thermal behavior between the tests were noted at the 350-mm elevation.

However, bundle size had a significant effect on maximum bundle temperatures and melt relocation behavior. The large PWR bundle test, CORA-7, showed substantially different melt relocation behavior than the other smaller PWR bundle tests. Unheated fuel rods at the 350-mm elevation, Figure 8, show no discontinuous changes in measured temperature response for CORA-7 while the other tests show a rapid rise in measured temperature due to the relocation of hot molten material from above. Lower radial heat losses in the larger bundle also resulted in a more rapid heatup particularly in the upper portion of the bundle with maximum temperatures exceeding 2100 K earlier than in small bundle tests. At the same time, maximum temperatures in the lower half of the CORA-7 bundle were reduced compared to smaller bundle tests due to the earlier reduction in power for CORA-7. As a result, the blockage region formed higher in the larger bundle.

The effects of bundle size in BWR experiments could not be ascertained directly from the available data since there was a relatively large difference in heating rates, and variations in coolant flow rates between CORA-16, 17, and 18. Coolant flow rates per rod used for the CORA-18 large bundle BWR experiment were considerably less than those used in the small bundle BWR tests, CORA-16 and 17. However, the coolant mass fluxes were larger in CORA-18 because of the differences in flow area associated with the control blade used in the three tests. The differences in flow rates affected the bundle heatup rate, and confounded the direct comparison of melt progression behavior. However, it can be assumed that behavioral influences because of bundle size were similar to those observed in PWR tests, because the power input to the heater rods was terminated at the same time as the large CORA-7 PWR test because of peak bundle temperatures exceeding 2100 K. Because the heatup behavior was similar to the large bundle PWR test, it can be assumed that the radial heat losses in the large bundle BWR test were lower than in the small bundle tests, resulting in faster heating of the bundle.

Ballooning of fuel rods from internal rod pressurization in the small CORA-15 bundle, resulted in behavior similar to the large bundle tests. Blockages occurred in the middle of the bundle because of the cooler region lower in the bundle. The causes of this cooler region were different than those in the large bundle tests but the effects on bundle damage were the same. Molten material, relocating from the hotter portions of the bundle, solidified quickly when coming in contact with cooler areas of the bundle and the partial blockage formed by fuel rod ballooning.

System Pressure

Because of the substantial differences in heating rate in the CORA-9 high system pressure test as compared to the other tests, the impact of a change in system pressure on melt progression behavior could not be determined. The high system pressure obviously impacted the thermal-hydraulics of the CORA-9 test, resulting in a substantially reduced heating rate with approximately the same initial conditions as other tests conducted at low pressure. However, reduced inlet temperatures as compared to other tests, in combination with outer shroud temperatures initially below saturation temperature, 458 K at 10-bar pressure, prohibited a clear interpretation of the CORA-9 thermal-hydraulic results, as well.

Slow Cooling Versus Rapid Quenching

When water was added to the CORA bundles to rapidly quench the bundle rather than slowly cooling the bundle in argon, additional heating, hydrogen production, and melting was observed during the reflood phase. Although the mechanisms causing such a response have not been clearly established, it is clear that the addition of water, while cooling the bundle as the quench front moves up through the bundle, resulted in additional oxidation and heat generation above the quench front. Thus the addition of water as compared to argon resulted in higher peak temperatures and more severe bundle damage, with the formation of additional liquefied material and the fragmentation of the bundle above regions of frozen material.

Unintentionally Varied Conditions or Experiment Uncertainties

The wide range of measured coolant temperatures at the inlet to the bundle for the CORA tests as shown on Figures 5 and 6 had little apparent effect on the outcome of the tests. Measured fuel rod temperatures at the 350-mm elevation and above were consistent for all tests. In particular, CORA-12 had one of the lower inlet temperatures but shows a bundle heatup comparable to other similar tests.

Variations in the coolant flow rate per rod was one of the most serious limitations in making direct comparisons between different tests. Different flow rates in CORA-2, the reference test, and CORA-18, the large bundle BWR test, limited direct comparison between these tests and other comparable PWR and BWR tests. In these tests with substantially reduced coolant flow rates per rod, oxidation driven bundle heatup occurred earlier and at a lower temperature than in the tests that had comparable coolant flows per rod or mass fluxes. These differences in bundle temperature response show that the flow rate and quantity of coolant per rod flowing through the bundle had a substantial effect on bundle heatup rates, temperatures at which rapid oxidation begins, and heat losses in the bundle. However, the changes in bundle heatup, oxidation, and melt relocation that may have resulted from differences in bundle size or configuration could not be separated from the influences of coolant flow.

Heat Losses

The interpretation of all the results in the tests were strongly influenced by uncertainties in radial heat losses. However, since most of the tests have similar heat losses as shown by similarities in bundle heatup rate, these uncertainties have a minimal impact on test-to-test comparisons. The two notable exceptions were the CORA-5 and CORA-9 tests. CORA-5 was the only test where the observation holes in the surrounding bundle shroud were filled by quartz windows. CORA-9 heat losses were altered by condensation on the outside of the shroud because of outer shroud temperatures starting initially below saturation temperature.

REFERENCES

1. S. HAGEN and K. HAIN, Out-of-Pile Bundle Experiments on Severe Fuel Damage (CORA Program): Objectives, Test Matrix, and Facility Description, KfK-3677 (1986).

2. S. HAGEN et al., "Out-of-Pile Experiments of Severe Fuel Damage Behavior of LWR Fuel Elements (CORA Program)," International Symposium of Severe Accidents in Nuclear Power Plants, Sorrento, Italy, March 1989, IAEA-SM-296/26.

3. S. HAGEN et al., "Out-of-pile Experiments in Meltdown Behavior of LWR Fuel Elements: Influence of (Ag,In,Cd) Absorber Material," International Conference on Thermal Reactor Safety, Avignon, France, October 1988.

4. C. M. ALLISON and E. C. JOHNSON (eds.), SCDAP/RELAP5/MOD2 Code Manual, Volumes I-III, NUREG/CR-5273, EGG-2555, September (1989).

5. S. HAGEN et al., "First Results of the CORA Tests, 9: High System Pressure, 7: Large PWR Bundle, 18: Large BWR Bundle," International CORA Workshop 90, Karlsruhe, Federal Republic of Germany, October (1990).

6. S. HAGEN, private communication.

7. T. J. HASTE and S. P. LOCK, "Posttest Analysis of CORA Experiments with SCDAP/RELAP5," International CORA Workshop '90, Karlsruhe, Federal Republic of Germany, October (1990).

8. P. HOFMANN, M. MARKIEWICZ, and J. SPINO, Reaction Behavior of B_4C Absorber Material with Stainless Steel and Zircaloy in Severe LWR Accidents, KfK-4598, July (1989).

9. K. MINATO, W. HERRING, and S. HAGEN, "Analysis of Zircaloy Oxidation and Cladding Deformation in CORA-2 and CORA-5," International CORA Workshop 90, Karlsruhe, Federal Republic of Germany, October (1990).

10. P. HOFMANN and M. MARKIEWICZ, Chemical Behavior of (Ag,In,Cd) Absorber Rods in Severe LWR Accidents, KfK-4670, August (1990).

11. S. HAGEN et al., Interactions in Zircaloy UO_2 Fuel Rod Bundles with Inconel Spacers at Temperatures above 1200°C (Posttest Results of Severe Fuel Damage Experiments CORA-2 and CORA-3), KfK-4378, September (1990).

12. W. HERRING, "Global Analysis of CORA Tests to Establish a Broad Data Base for Calculation," International CORA Workshop-3, Karlsruhe, Federal Republic of Germany, September (1989).

END

DATE FILMED

01/06/92